Supporting Information

Sutherland et al. 10.1073/pnas.1319963111

SI Materials and Methods

Histology and Immunohistochemistry. For histological analysis, lungs were inflated with ethanol–acetic acid–formalin (EAF) and fixed for 24 h in EAF. Fixed tissues were subsequently dehydrated, embedded in paraffin, and sections (4 μm) prepared and stained by hematoxylin and eosin (H&E). For immunohistochemistry, tissue sections were rehydrated, blocked in BSA containing PBS, and sequentially incubated with specific primary antibodies and with biotinylated secondary antibodies (DAKO). Streptavidin-peroxidase (DAKO) or Powervision Poly-HRP (Leica Microsystems) was used for visualization and diaminobenzidine as a chromagen (DAKO). The following antibodies were used: anti-Clara cell antigen 10 (CC10) (goat polyclonal, 1:5,000), anti-high mobility group AT-hook 2 (Hmga2) (rabbit polyclonal, 1:1,000, BioCheck: 59170AP), anti-NK2 homeobox 1 (Nkx2-1) (mouse monoclonal, 1:1,000), anti–pro-Surfactant Protein C (SPC) (rabbit polyclonal, 1:2,000, Chemicon), and anti-sex determining region Y-box 2 (Sox2) (rabbit polyclonal, 1:1,000, Millipore).

Immunofluorescence Microscopy. For immunofluorescence microscopy, Ad5–Cre-infected *K-Ras*$^{\text{lox-Stop-lox-G12D/+}}$ lungs were inflated and fixed with EAF overnight. Fixed lungs were embedded in paraffin. For immunofluorescence, tissue sections were rehydrated, blocked in normal donkey serum containing PBS/0.2% tween-20, and incubated with specific primary antibodies and with Alexa Fluor-coupled secondary antibodies. Paraffin sections were stained with the following primary antibodies: goat anti-CC10 (1:200; Santa Cruz: sc-9972) and rabbit anti–pro-SPC (1:1,000; Chemicon; AB3786). Alexa Fluor-coupled secondary antibodies (Invitrogen) were used at a 1:200 dilution. Images were captured on a Leica SP5C Spectral Confocal Laser Scanning Microscope.

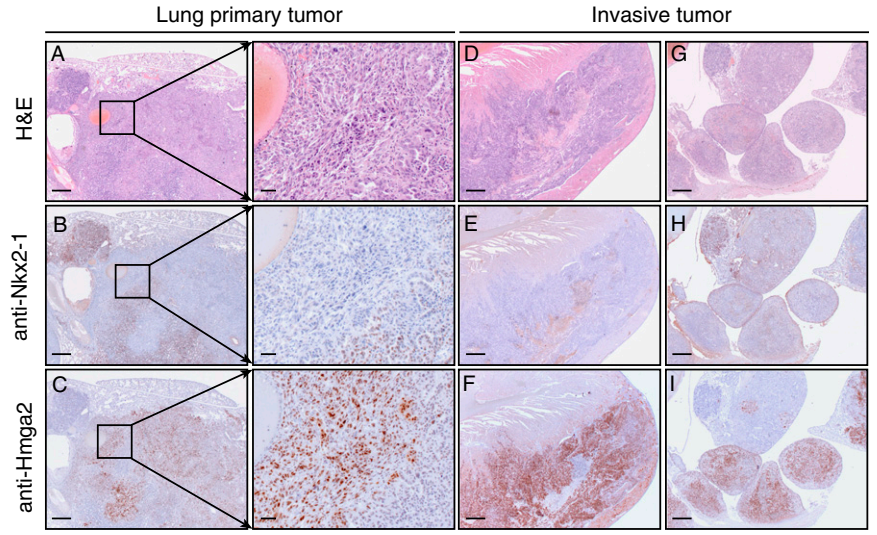

Fig. S1. Poorly differentiated and invasive lung tumors exhibit high Hmga2 expression. (*A*–*C*) Microphotographs of serial sections of a representative poorly differentiated lung carcinoma from a *K-Ras*$^{\text{LSL-G12D/+}}$;tumor suppressor gene p53 (*Trp53*)$^{\text{F/F}}$ mouse examined 177 d following Ad5–CC10–Cre infection. (*A*) H&E-stained section showing pleomorphism of the tumor with the areas of necrosis and poor differentiation such as spindle cell transformation and trabecular and irregular glandular structures (*Inset*). Immunostainings of Nkx2-1 (*B*) and Hmga2 (*C*) showing complementary staining patterns in the areas of poor differentiation with no Nkx2-1 staining that is accompanied by strong staining of Hmag2 (*Insets*). (*D*–*F*) Micrographs of serial sections of an invasive lung carcinoma in myocardium from a *K-Ras*$^{\text{LSL-G12D/+}}$;*Trp53*$^{\text{F/F}}$ mouse examined 177 d following Ad5–CC10–Cre infection. (*D*) H&E staining. Immunostainings of Nkx2-1 (*E*) and Hmga2 (*F*) showing negative staining of Nkx2-1 but strong positive staining of Hmga2. (*G*–*I*) Microphotographs of serial sections of an invasive lung carcinoma in the thoracic cavity from a *K-Ras*$^{\text{LSL-G12D/+}}$;*Trp53*$^{\text{F/F}}$ mouse analyzed 177 d following Ad5–CC10–Cre infection. (*D*) H&E staining. Immunostainings of Nkx2-1 (*H*) and Hmga2 (*I*) showing negative staining of Nkx2-1 but strong positive staining of Hmga2. (Scale bar in *A*–*C*, 500 μM; *Insets*, 50 μM; *D*–*I*, 500 μM.)

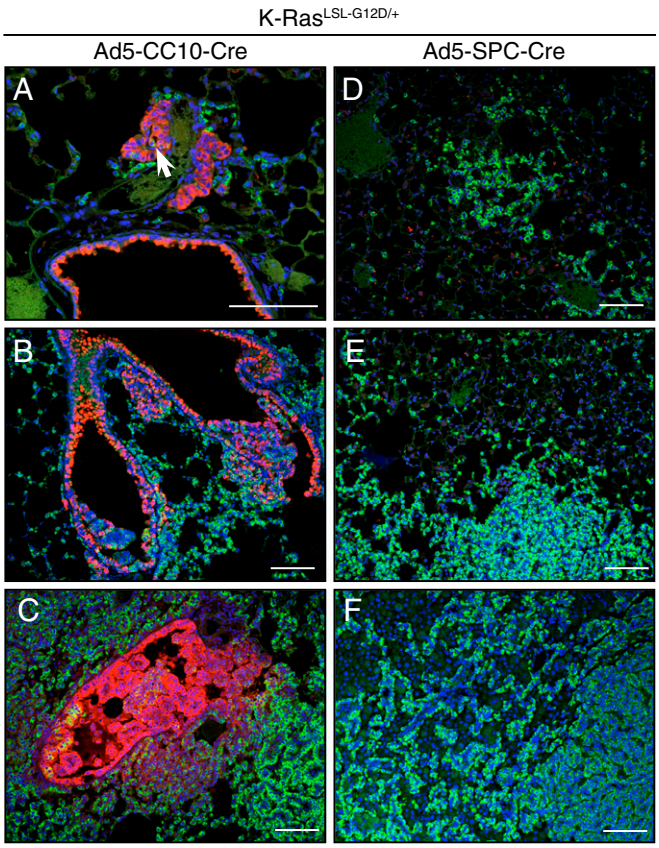

Fig. S2. Bronchioalveolar stem cells (BASCs) are not the sole cancer-initiating cell of K-RasG12D–induced transformation. (*A*–*C*) Sections of *K-Ras*$^{LSL-G12D/+}$ mouse lungs at various stages following Ad5–CC10–Cre infection were stained with anti-CC10 (red) and pro-SPC (green). (*A*) Coimmunofluorescence (co-IF) staining of initial lesions detects rare CC10^{+}SPC^{+} cells (arrows) at the bronchioalveolar duct junction (BADJ). (*B*) Papillary hyperplasia at the BADJ consists of rare CC10^{+}SPC^{+} BASCs and CC10- and SPC single-positive cells. (*C*) Bronchiolar and alveolar hyperplasia stain positive for CC10 and pro-SPC, respectively. (*D*–*F*) A time course of adenocarcinoma progression in *K-Ras*$^{LSL-G12D/+}$ mice following Ad5–SPC–Cre infection shows no involvement of CC10^{+}SPC^{+} BASCs following K-RasG12D activation in SPC-expressing cells. (*D*) Alveolar hyperplasia consists of SPC^{+} cells. (*E*) Normal BADJ (arrow) and SPC^{+} alveolar adenomatous hyperplasia in the periperal lung and (*F*) an SPC^{+} adenocarcinoma. (Scale bar in *A*, 50 μM; *B*–*F*, 100 μM.)

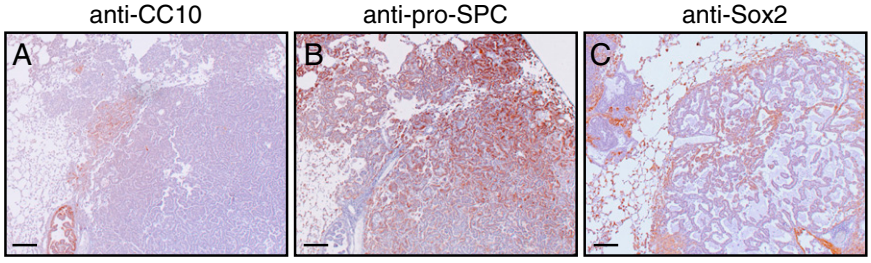

Fig. S3. Sox2 expression is partially lost in more progressed lesions. Immunohistochemical staining of lung tissue sections from a *K-Ras*$^{LSL-G12D/+}$ mouse 491 d following Ad5–CC10–Cre infection. (*A*) Staining for the Clara cell maker, CC10; (*B*) staining for the alveolar type 2 cell marker, pro-SPC; and (*C*) staining for Sox2. (Scale bar in *A*–*C*, 200 μM.)

Table S1. Overview of the number of *K-Ras*$^{LSL-G12D/+}$ mice subjected to the experiment

	K-Ras$^{LSL-G12D/+}$ mice	
	Adenovirus	
Time point, wk	Ad5–SPC–Cre	Ad5–CC10–Cre
8	4	4
12	5	3
18	5	7
24	5	4
32	3	4
32–88	5	8

Table S2. Overview of the number of *K-Ras*$^{LSL-G12D/+}$;*Trp53*$^{F/F}$ mice subjected to the experiment

	K-Ras$^{LSL-G12D/+}$;*Trp53*$^{F/F}$ mice	
	Adenovirus	
Time point, wk	Ad5–SPC–Cre	Ad5–CC10–Cre
4	4	4
8	3	3
18	2	6
18–46	8	9